POLITECNICO
MILANO 1863

SCUOLA DI INGEGNERIA INDUSTRIALE
E DELL'INFORMAZIONE

EXECUTIVE SUMMARY OF THE THESIS

A Computational Framework for Longitudinal Airway Analysis in Chronic Hypersensitivity Pneumonitis

TESI MAGISTRALE IN BIOMEDICAL ENGINEERING – INGEGNERIA BIOMEDICA

AUTHOR: MARTINO GHEZZI

ADVISOR: FRANCESCA PENNATI - CO-ADVISOR: ANDREA ALIVERTI

ACADEMIC YEAR: 2024-2025

Abstract

Chronic hypersensitivity pneumonitis (CHP) is an interstitial lung disease that involves highly variable inflammatory–fibrotic remodeling and unpredictable longitudinal trajectories. Its clinical follow-up still relies mainly on global spirometric indices such as forced vital capacity (FVC) [1]. This work presents a fully reproducible computational pipeline to quantify longitudinal airway geometric changes from chest HRCT and relate them to functional and parenchymal variations in CHP. The framework includes airway/lung/lobe segmentation, extraction of airway measurements, longitudinal registration between timepoints, and cohort-level statistical analysis. The dataset included longitudinal inspiratory HRCT and spirometry from fibrotic CHP patients. Each longitudinal pair was stratified by ΔFVC into Improving, Stable, and Worsening groups. Intensity and geometrical variations were computed both at a global (whole-lung) and local (lobar) level.

Registration validation reached a median target registration error of 1.50 mm (IQR 0.96–2.07 mm). Global analysis showed a clear separation in mean lung density change (ΔHU), whereas global airway geometry alone was less discriminative; lobar analysis revealed strong associations between ΔHU and airway metrics, highlighting distinct and heterogeneous remodeling patterns across groups. Overall, the pipeline enables spatially resolved quantitative assessment of airway remodeling beyond spirometry and supports complementary CT-derived intensity and geometry biomarkers for CHP monitoring.

1. Introduction

Hypersensitivity Pneumonitis (HP) is a heterogeneous interstitial lung disease (ILD) caused by the inhalation of specific organic antigens or low-weight molecular substances that trigger an exaggerated immune response in susceptible individuals [2]. Repeated or continuous exposure may induce a hypersensitivity response characterized by persistent epithelial injury and an aberrant immune response, ultimately leading to fibroblast activation, collagen deposition, interstitial

remodelling, and fibrosis [3]. This disease is traditionally classified into three clinical forms according to the duration of the symptoms: acute, sub-acute, and chronic. The latter, named Chronic Hypersensitivity Pneumonitis (CHP), is the final stage of the disease, which develops over months or years. It leads to irreversible fibrotic changes that persist or progress even after the removal of the antigen [3].

The diagnosis of the disease relies on a comprehensive multidisciplinary assessment that integrates detailed exposure history, clinical evaluation, imaging, and, eventually, bronchoalveolar lavage (BAL) and transbronchial biopsy findings. Radiologic assessments are the most important ones, as high-resolution computed tomography (HRCT) allows the identification of a broad range of parenchymal patterns. These reflect airway, interstitial, and alveolar involvement, contributing to disease characterization and phenotypic stratification [3].

Currently, the gold standard for longitudinal assessment is spirometry, with particular emphasis on forced vital capacity (FVC) [1]. Unfortunately, it presents several limitations: it provides a global measure of the disease, and is relatively insensitive to regional disease progression, which may be masked by compensatory mechanisms in other lung regions and to small changes in the pathology. Due to these reasons, automated methods of image analysis are gaining importance in this field. Aliboni et al. [1] developed an automatic convolutional neural network (CNN) algorithm to objectively quantify the presence of specific CHP patterns.

Following these recent trends, trying to analyse CHP pathology from a quantitative point of view starting from the HRCT images, the goal of this thesis is to provide a replicable pipeline to evaluate airway geometrical variations in pathological patients over time.

2. Materials and Methods

The overall pipeline can be subdivided into 4 stages: the first three are related to the registration framework, while the fourth refers to its evaluation on a CHP dataset.

2.1. Segmentation phase

The Segmentation phase produces the lungs', lobes' and airways' masks. The first two objects are retrieved through the TotalSegmentator algorithm [4]. These segmentations don't need to be extremely precise as they are used to initialize the registration step and to allow the assignement of the measurement points to specific lobes.

In contrast, airway tree segmentation requires much finer segmentation tools, as geometrical measurements are performed on these objects. In order to achieve this goal, existing airway segmentation challenges were reviewed. The final choice fell into the top-performing methods from the "Airway Tree Modelling 2022" challenge [5]. The first classified code ("team timi") had reproducibility issues in our environment, so the second classified one ("team Yang") was selected for this study. An example of resulting airway segmentation is shown in Figure 2.1.

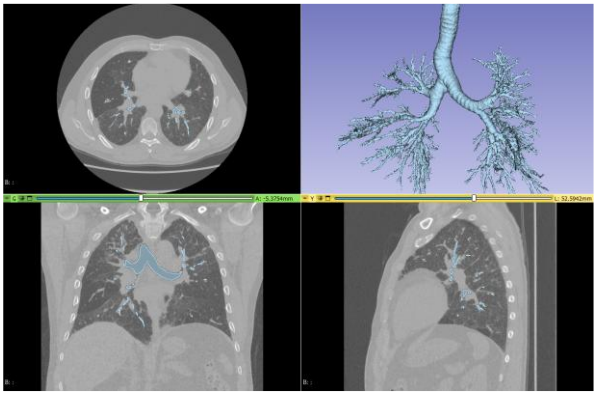

Figure 2.1 : Example of airway tree segmentation using "team Yang" algorithm [5].

2.2. Measurement phase

The Measurement phase can be performed in parallel with the registration one, as they both require the airway segmentations and the original HRCT scans as input. The original algorithm developed by Mascheroni et al. [6] was slightly modified to optimize performance for the present application. The following geometrical measurements were extracted: total area, edge area, lumen area, mean and std dev of wall thickness, inner major and minor axes, outer major and minor axes. Those parameters were calculated at each measurement point (decided by the user) on every branch of the airway tree skeletonization. The user selects the points along each branch based

on a normalized curvilinear coordinate ranging from 0 and 1, where 0 corresponds to the proximal end and 1 to the distal end of the branch.

For each selected location, the algorithm computes the airway cross-section. Local airway direction is estimated from the centreline using two neighbouring points (one proximal and one distal to the measurement point). A plane orthogonal to this local direction is defined, and the intersection between this plane and the airway mask yields the corresponding cross-section. This procedure is repeated for each point of measurement.
The curvilinear coordinate is set around the center of the branches, slightly shifted towards the distal regions (60% of the branches). If the measurement point is too close to the proximal bifurcation, the cross-sectional plane may intersect two partially connected daughter airways, that are not yet fully separated in the segmentation mask, leading to inaccurate geometrical estimates.

In addition to cross-sectional measurements, branching points of the airway skeleton are extracted. These landmarks are used in the validation phase of the registration process.

2.3. Registration phase

The registration process aims to find the correspondence between measurement points in longitudinal pairs of HRCTs. It allows the computation of geometrical variations over time. The process is organized into three steps: affine registration, deformable registration, and validation.

Affine registration. The affine registration establishes an initial global alignment between the two time points. The alignment was not performed directly on the airway trees, due to their structural complexity and variability across time points. It is instead performed on the lung masks. In such a way, the initial alignment provides a more robust and reliable initialization for the subsequent deformable step.

Deformable Registration. The deformable registration, initialized with the affine transformation estimated before, is computed on the original HRCTs volumes after an airway intensity saturation to enhance structural consistency. A diffeomorphic demons algorithm was chosen, which appeared to be best on this type of application.

Validation. The estimated transformations are applied to the branching points extracted from the moving image, and their correspondence with branching points in the fixed image is evaluated using the closest point approach. The target registration error (TRE) is calculated as the Euclidean distance between matched landmarks. A critical issue arises from the fact that the number and lengths of the segmented branches often differ between time points. Consequently, not all branching points in the fixed segmentation have true anatomical correspondences in the moving segmentation, and vice versa. As a solution to this problem, for validation purposes only, the fixed image was reconstructed using a standard "lung" kernel, while the moving image was reconstructed using a "body" kernel. The coarser reconstruction of the moving image leads to a shallower airway segmentation, increasing the likelihood that all moving branching points are included within the fixed set. In this configuration, each moving branching point is matched to its nearest fixed neighbour, while unmatched fixed points are allowed.
This strategy avoids the arbitrary exclusion of branching points based only on a distance threshold, which could alter the TRE results by confusing true anatomical differences with registration errors.
An example of a successful registration process is shown in Figure 2.2.

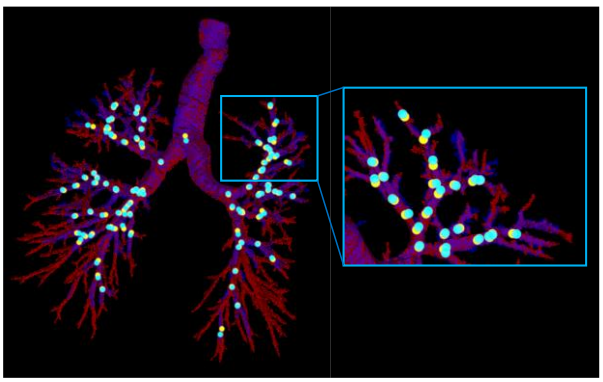

Figure 2.2 : Fixed (red) and moving deformed (blue) airway segmentations superimposed and their corresponding branching points matched.

2.4. Evaluation on CHP dataset

Dataset

The dataset is composed by noncontrast-enhanced, inspiratory chest CT performed for a cohort of 27 fibrotic HP patients. Patients were scanned on a Brilliance 16P scanner (Philips Medical Systems, Andover, MA), from lung apices to bases, at full inspiration, after standardized breathing instructions, using a weight-based CT technique for dose minimization. The imaging parameters were: tube voltage around 120-140 kVp, tube current set to 30 mAs, pixel matrix of dimension 512x512, slice thickness of 0.8-1 mm and two types of reconstruction filter ("body" and "lung").

Statistical analysis

The developed pipeline was applied to the CHP dataset, with the aim of identifying common remodeling patterns in terms of geometrical variations over time. Longitudinal changes were calculated at corresponding measurement points and expressed as percentage variations and averaged at both the whole-lung and lobar levels, allowing both global and regional analysis. The global analysis uses patient-level aggregated metrics, including total ΔFVC, total lung ΔHU, and the median percentage change of airway geometrical features. Descriptive statistics were reported and results were visualized using box plots. When distributional assumptions were satisfied, group comparisons were performed using parametric tests with a significance level set at $\alpha = 0.05$. The local analysis uses lobar segmentation to compute mean lobar ΔHU and mean percentage variation of airway geometrical parameters per lobe. Associations between regional densitometric changes and airway remodeling were explored.

Finally, longitudinal FVC variations was also used to subdivide the dataset into three subsets: improving patients (ΔFVC > 5%), stable patients (|ΔFVC| <= 5%), and worsening patients (ΔFVC < 5%).

3. Results and Discussion

3.1. Dataset reduction

After reviewing the complete dataset, a substantial number of subjects were discarded due to predefined quality criteria (missing images/spirometry, images acquired in prone positioning, in-plane resolution differences larger than 0.1 mm, and a slice thickness greater than 0.8 mm. For these reasons, the initial dataset of 27 patients was reduced to 9 eligible subjects, with 1–4 image pairs per patient. All image pairs were then classified according to ΔFVC into stable, worsening, or improving groups.

3.2. Validation results

Across the tested registration strategies, the initial TRE before any transformation was 150.72 mm (median), with an interquartile range (IQR) of 138.55-168.23 mm. After the initial affine alignment, TRE decreased to 6.76 mm (median), with an IQR of 5.31-8.45 mm. Finally, after optimization of affine and deformable parameters, TRE reached 1.50 mm (median), with an IQR of 0.96-2.07 mm. Considering a slice thickness of 0.8 mm, the final mean registration error corresponds to approximately 2 voxels along the z-axis, which is considered acceptable for longitudinal analysis.

3.3. Global analysis

As it can be seen in Figure 3.1 and in Figure 3.2, a clear separation between the three groups emerged in terms of mean global ΔHU, confirming the consistency between functional and densitometric metrics:

- The Improving group had mainly negative ΔHU values (reduction of the mean lung density).
- The Stable group had small variations centered around zero.
- The Worsening group had only positive ΔHU (increase in mean lung density).

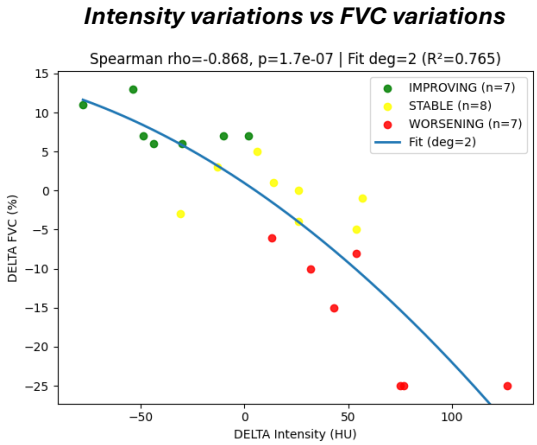

Figure 3.1 : Boxplot of mean global ΔHU in the three FVC-based groups. * p ≤ 0.05, ** p ≤ 0.01, *** p ≤ 0.001.

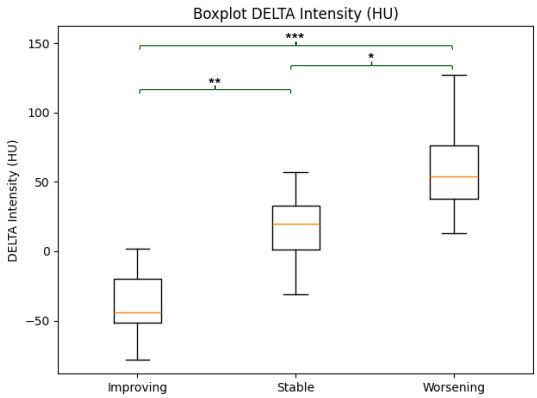

Figure 3.2 : Relationship between ΔFVC and global ΔHU.

Global geometrical variations were also evaluated:

- The Improving group showed mainly positive percentage variations across most geometrical measures (increase in total, lumen, and edge areas).
- The Stable group exhibited variations centered around small values close to zero.
- The Worsening groups showed variations also centered near zero, with slightly more negative values in some parameters.

Despite these observable trends, none of the global geometrical parameters reached statistical significance between groups (all p-values > 0.05), as can be seen in Table 3.1. This reflects disease heterogeneity, which makes some regions of the lungs more affected by a specific pattern, while others are more affected by different ones.

3.4. Local analysis

Given the limited discriminative power of global geometrical metrics, a regional (lobar) analysis was performed to explore potential spatial associations between local density changes and airway remodeling (including areas and axis variations):

- In the Improving group a steep, and significant inverse relationship was observed: decreasing density was associated with increasing airway areas. This suggests that airway expansion may accompany a decrease in lung inflammation.
- The Stable group exhibited a weak or absent monotonic association, especially considering the lumen area, indicating limited structural remodeling over time.
- The Worsening group showed a better inverse relationship considering total and lumen area in particular, even though with a different steepness with respect to the first group.

	IMPROVING (median [IQR])	**STABLE** (median [IQR])	**WORSENING** (median [IQR])	**p-value**
Δ Total area (%)	17.45 [27.21]	4.13 [6.47]	3.03 [13.94]	0.30
Δ Edge area (%)	11.49 [16.44]	1.34 [7.93]	0.00 [10.10]	0.31
Δ Lumen area (%)	24.66 [34.64]	8.05 [9.22]	5.56 [14.84]	0.24
Δ Inner Major Axis (%)	8.41 [16.20]	2.88 [4.77]	2.70 [4.26]	0.34
Δ Inner Minor Axis (%)	11.26 [13.86]	1.78 [4.41]	1.82 [6.46]	0.24
Δ Outer Major Axis (%)	7.23 [11.78]	1.83 [5.43]	2.05 [4.11]	0.33
Δ Outer Minor Axis (%)	7.92 [10.89]	1.04 [3.42]	1.50 [5.34]	0.31

Table 3.1 : Global analysis. Median and interquartile range values for different measurements' variations in the three groups.

	IMPROVING	STABLE	WORSENING
ΔHU vs ΔTotal area	-0.70 (p=3.23e-06)	-0.37 (p=2.02e-02)	-0.64 (p=3.01e-05)
ΔHU vs ΔEdge area	-0.68 (p=8.57e-06)	-0.53 (p=4.83e-04)	-0.51 (p=1.72e-03)
ΔHU vs ΔLumen area	-0.69 (p=4.58e-06)	-0.28 (p=7.91e-02)	-0.61 (p=1.06e-04)
ΔHU vs ΔInner Major Axis	-0.69 (p=4.00e-06)	-0.28 (p=8.10e-02)	-0.48 (p=3.6e-03)
ΔHU vs ΔInner Minor Axis	-0.71 (p=1.97e-06)	-0.30 (p=5.79e-02)	-0.53 (p=9.74e-04)
ΔHU vs ΔOuter Major Axis	-0.69 (p=4.60e-06)	-0.35 (p=2.89e-02)	-0.53 (p=1.0e-03)
ΔHU vs ΔOuter Minor Axis	-0.73 (p=5.64e-07)	-0.50 (p=1.08e-03)	-0.60 (p=1.56e-04)

Table 3.2 : Local analysis. Spearman correlations between lobar longitudinal changes (ΔHU and ΔMeasurement) in three groups; p-values are provided.

However, the pattern was more complex as increases in density were associated with mixed airway responses. In some cases, airway dimensions decreased, consistent with progressive fibrotic narrowing; in others modest airway enlargement was observed, possibly reflecting traction bronchiectasis secondary to fibrosis.

Quantitative local results are listed in Table 3.2.

4. Conclusion

The proposed pipeline provides a reproducible framework for longitudinal quantitative airway analysis in CHP. Global lung density variations clearly separate Improving, Stable, and Worsening subjects. In contrast, global geometric metrics alone were insufficient to separate groups. At the regional level, meaningful associations between density variation and airway remodeling emerged.

Several limitations must be acknowledged. The dataset was limited and heterogeneous in baseline FVC and lung density, preventing stratified analyses; minor variability in acquisition parameters may have added noise, and lobar-level analysis may still average heterogeneous patterns, suggesting that a finer (segmental) approach could be useful. Methodologically, segmentation was chosen qualitatively, measurements were computed at discrete points, and registration was validated on coarser reconstructions, so future work should include larger cohorts, quantitative model comparisons, branch-level metrics, and machine learning-based pattern-recognition, with potential extension beyond CHP to other fibrotic diseases and translational applications.

5. Bibliography

References

[1] L. Aliboni *et al.*, 'A Convolutional Neural Network Approach to Quantify Lung Disease Progression in Patients with Fibrotic Hypersensitivity Pneumonitis (HP)', *Acad. Radiol.*, vol. 29, no. 8, pp. e149–e156, Aug. 2022, doi: 10.1016/j.acra.2021.10.005.

[2] M. Hamblin, H. Prosch, and M. Vašáková, 'Diagnosis, course and management of hypersensitivity pneumonitis', *Eur. Respir. Rev.*, vol. 31, no. 163, p. 210169, Mar. 2022, doi: 10.1183/16000617.0169-2021.

[3] O. M. Dias *et al.*, 'Computed tomography in hypersensitivity pneumonitis: main findings, differential diagnosis and pitfalls', *Expert Rev. Respir. Med.*, vol. 12, no. 1, pp. 5–13, Jan. 2018, doi: 10.1080/17476348.2018.1395282.

[4] J. Wasserthal *et al.*, 'TotalSegmentator: Robust Segmentation of 104 Anatomic Structures in CT Images', *Radiol. Artif. Intell.*, vol. 5, no. 5, p. e230024, Sep. 2023, doi: 10.1148/ryai.230024.

[5] M. Zhang *et al.*, 'Multi-site, Multi-domain Airway Tree Modeling', *Med. Image Anal.*, vol. 90, p. 102957, Dec. 2023, doi: 10.1016/j.media.2023.102957.

[6] C. Mascheroni, 'Automatic measurement of airway dimensions from CT images in health and asthma', Politecnico di Milano, 2022.